

Search for Higgs boson decay to a charm quark-antiquark pair via $t\bar{t}H$ production

Sebastian Wuchterl
on behalf of the CMS Collaboration^a
*CERN, Espl. des Particules 1,
1211 Meyrin, Switzerland*

In these proceedings, a search for the standard model Higgs boson decaying to a charm quark-antiquark pair, $H \rightarrow c\bar{c}$, produced in association with a top quark-antiquark pair ($t\bar{t}H$) is presented. The search is performed using proton-proton collision data collected by the CMS experiment at $\sqrt{s} = 13$ TeV, corresponding to an integrated luminosity of 138 fb^{-1} . The Higgs boson decay to a bottom quark-antiquark pair is measured simultaneously and the observed $t\bar{t}H(H \rightarrow b\bar{b})$ event rate relative to the standard model expectation is found to be $0.91^{+0.26}_{-0.22}$. The observed (expected) upper limit at 95% confidence level (CL) for $t\bar{t}H(H \rightarrow c\bar{c})$ production is 7.8 (8.7) times the standard model prediction. Combined with a previous search for $H \rightarrow c\bar{c}$ via associated production with a W or Z boson, the observed (expected) 95% CL interval on the Higgs-charm Yukawa coupling modifier, κ_c , is $|\kappa_c| < 3.5$ ($|\kappa_c| < 2.7$).

1 Introduction

The discovery of a Higgs boson (H) by the ATLAS¹ and CMS² experiments in 2012^{3,4} marks a milestone in understanding the electroweak symmetry breaking. With a measured mass of $125.38 \pm 0.14 \text{ GeV}$ ⁵, the observed interactions with gauge bosons and third-generation fermions, as well as all measured properties of the Higgs boson, agree with standard model (SM) predictions^{6,7}. Following the first evidence of Higgs boson decays to muons⁸, an important next step is the observation of the Higgs boson coupling to second-generation quarks. Searches for Higgs boson decays to a charm quark-antiquark pair ($c\bar{c}$) provide direct access to the charm Yukawa coupling (y_c). Using 138 fb^{-1} of proton-proton collision data at 13 TeV, the ATLAS⁹ and CMS¹⁰ Collaborations reported observed (expected) 95% confidence level (CL) intervals on $\kappa_c = y_c/y_c^{\text{SM}}$ of $|\kappa_c| < 4.2$ (4.1) and $1.1 < |\kappa_c| < 5.5$ ($|\kappa_c| < 3.4$), respectively, studying the associated production of a Higgs boson with a V (W or Z) boson. These proceedings report a new search for $H \rightarrow c\bar{c}$ via associated production of a Higgs boson with a top quark-antiquark pair ($t\bar{t}H$), while the $H \rightarrow b\bar{b}$ decay is measured simultaneously. In addition, the SM processes $t\bar{t}Z(Z \rightarrow c\bar{c})$ and $t\bar{t}Z(Z \rightarrow b\bar{b})$ are measured to validate the analysis strategy for $t\bar{t}H$ production.

2 Analysis strategy

The analysis uses proton-proton collision data at $\sqrt{s} = 13$ TeV, collected by the CMS detector and corresponding to an integrated luminosity of 138 fb^{-1} and is carried out in three channels targeting the fully hadronic (0L), semileptonic (1L), and dileptonic (2L) decays of the $t\bar{t}$ pair. To identify the jet flavor, the ParticleNet algorithm¹¹ is used. Two discriminants are defined

^aCopyright [2024] CERN for the benefit of the CMS Collaboration. Reproduction of this article or parts of it is allowed as specified in the CC-BY-4.0 license

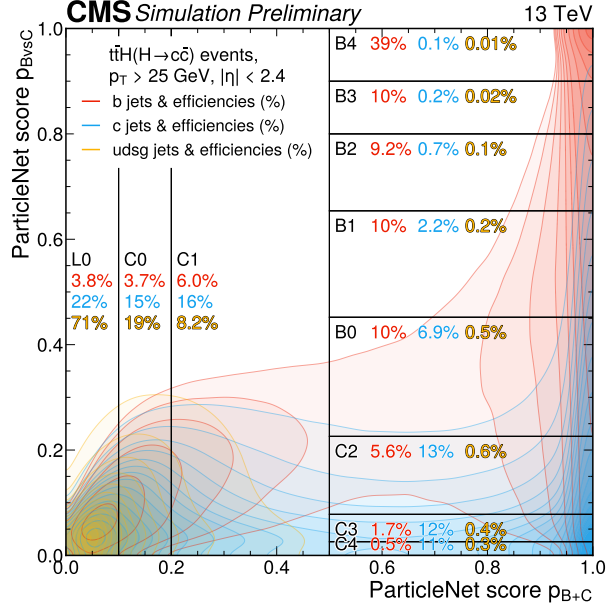


Figure 1 – Distribution of b, c and light-flavor jets in the two-dimensional ParticleNet discriminant plane, together with the tagging categories and the corresponding efficiencies¹³.

from the ParticleNet outputs: p_{B+C} , which separates heavy- from light-flavor jets, and p_{BvsC} , which distinguishes b from c jets. Based on these, 11 mutually exclusive tagging categories are defined as shown in Fig. 1. Compared to the previous tagging algorithm used in the CMS Collaboration, DEEPJET¹², ParticleNet improves the b vs. light and c vs. b jet rejection by up to a factor of two each at the same signal jet efficiency.

A multiclass event classifier based on ParT¹⁴ is developed to classify events. The ParT classifier is a transformer based algorithm which combines inputs such basic kinematic properties and tagging information with pairwise features for all object pairs derived using their four-momenta to better learn the event kinematic properties and object correlations. The classifier is trained to assign likelihood scores across 10 (9) classes in the 0L (1L, 2L) channel: two $t\bar{t}H$ classes ($t\bar{t}H(H \rightarrow c\bar{c})$, $t\bar{t}H(H \rightarrow b\bar{b})$), two $t\bar{t}Z$ classes ($t\bar{t}Z(Z \rightarrow c\bar{c})$, $t\bar{t}Z(Z \rightarrow b\bar{b})$), five $t\bar{t}$ +jets classes ($t\bar{t}+b$, $t\bar{t}+\geq 2b$, $t\bar{t}+c$, $t\bar{t}+\geq 2c$, $t\bar{t}+\text{light}$), and only in the 0L channel, one class for QCD multijet.

The output scores of the ParT classifier are used to optimize the event selection and categorization. In the 0L channel, a stringent requirement on the QCD multijet score suppresses this background by about four orders of magnitude, making it negligible compared to $t\bar{t}$ +jets. Similarly, a selection on the $t\bar{t}$ +light discriminant further reduces $t\bar{t}$ +light contamination in all channels. Only events with a high $t\bar{t}H$ or $t\bar{t}Z$ score value are retained for the signal extraction and background estimation. Events passing these criteria are categorized into four signal regions (SRs), enriched in $t\bar{t}H(H \rightarrow c\bar{c})$, $t\bar{t}H(H \rightarrow b\bar{b})$, $t\bar{t}Z(Z \rightarrow c\bar{c})$, and $t\bar{t}Z(Z \rightarrow b\bar{b})$, together with five control regions (CRs), to estimate the normalizations of the $t\bar{t}$ +jets background components.

The $t\bar{t}H$ and $t\bar{t}Z$ production rates are determined via a binned profile likelihood fit to data. For each of the four signal processes, the expected yield is scaled by a signal strength modifier μ , defined as $(\sigma\mathcal{B})_{\text{obs}} / (\sigma\mathcal{B})_{\text{SM}}$ where σ is the production cross section and \mathcal{B} is the branching fraction of the H or Z decays. The dominant background, $t\bar{t}$ +jets, is estimated with the normalizations of the $t\bar{t}+c$, $t\bar{t}+\geq 2c$, $t\bar{t}+b$, $t\bar{t}+\geq 2b$, and $t\bar{t}$ +light components floating independently and constrained in dedicated control regions. For $\mu_{t\bar{t}H(H \rightarrow c\bar{c})}$, the leading uncertainty is statistical ($\approx 74\%$), whereas for $\mu_{t\bar{t}H(H \rightarrow b\bar{b})}$, the largest uncertainties are theoretical in the $t\bar{t}$ +jets model, representing $\approx 60\%$ of the total uncertainty.

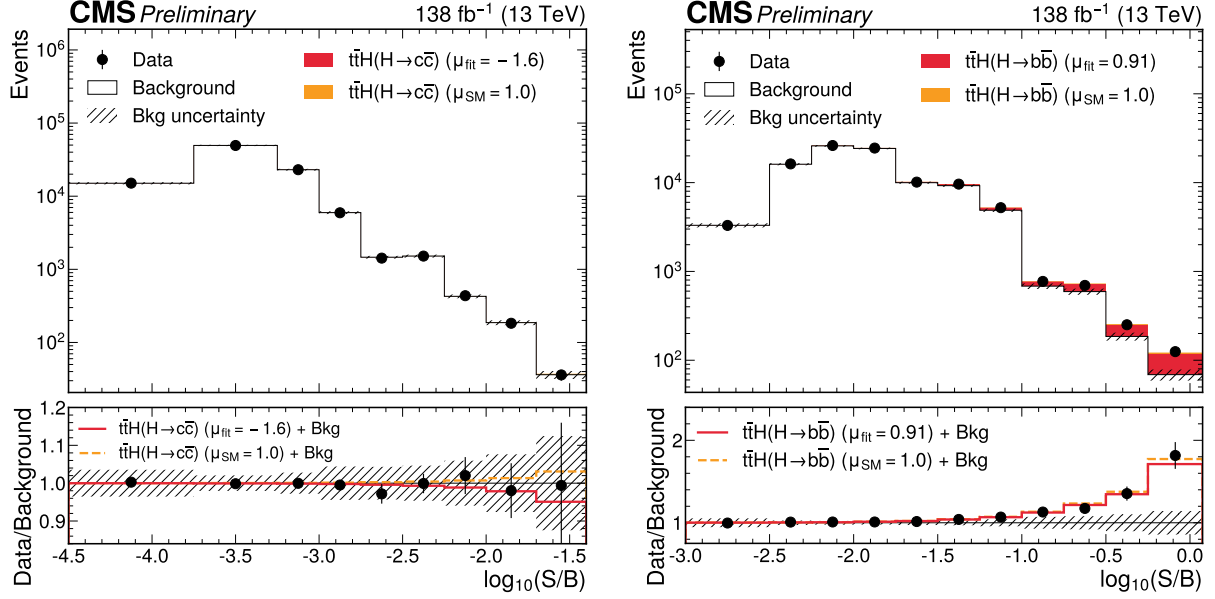


Figure 2 – Observed and expected event yields from all SRs and CRs as a function of $\log_{10}(S/B)$, where S are the expected $t\bar{t}H(H \rightarrow c\bar{c})$ (left) and $t\bar{t}H(H \rightarrow b\bar{b})$ (right) yields, and B are the post-fit total background yields. Signal contributions are shown for the best-fit signal strength (red) and for the SM prediction, $\mu = 1$ (orange). The lower panel shows the ratio of the data to the post-fit background predictions¹³.

3 Results

The analysis is validated by measuring the $t\bar{t}Z$ signal strengths $\mu_{t\bar{t}Z(Z \rightarrow c\bar{c})} = 1.02^{+0.79}_{-0.84}$ and $\mu_{t\bar{t}Z(Z \rightarrow b\bar{b})} = 1.47^{+0.45}_{-0.41}$, which agree with the SM prediction within one (two) standard deviation for the $Z \rightarrow c\bar{c}$ ($Z \rightarrow b\bar{b}$) decay mode, and with measurements in the leptonic decay channel^{15,16}.

Figure 2 shows the observed and expected event yields from all CRs and SRs as a function of the logarithm of the ratio of $t\bar{t}H(H \rightarrow c\bar{c})$ (or $t\bar{t}H(H \rightarrow b\bar{b})$) and background yields. The best-fit signal strengths for $t\bar{t}H$ production are determined to be $\mu_{t\bar{t}H(H \rightarrow c\bar{c})} = -1.6 \pm 4.5$ and $\mu_{t\bar{t}H(H \rightarrow b\bar{b})} = 0.91^{+0.26}_{-0.22}$, with an observed (expected) significance of 4.4 (4.5) standard deviations for $t\bar{t}H(H \rightarrow b\bar{b})$. An upper limit on $\mu_{t\bar{t}H(H \rightarrow c\bar{c})}$ is extracted using the CLs criterion, with an observed (expected) 95% CL upper limit on $\mu_{t\bar{t}H(H \rightarrow c\bar{c})}$ of 7.8 (8.7).

The result is interpreted in the κ -framework¹⁷ by parameterizing $\mathcal{B}(H \rightarrow c\bar{c})$ and $\mathcal{B}(H \rightarrow b\bar{b})$ in terms of the charm and bottom quark Yukawa coupling modifiers κ_c and κ_b . Figure 3 shows the two-dimensional profile likelihood scan of κ_c and κ_b . When fixing κ_b to the SM expectation of unity, the observed (expected) 95% CL interval is $|\kappa_c| < 3.0$ (3.3).

Finally, a combined analysis with the previous search in the VH channel¹⁰ is performed. The observed (expected) 95% CL upper limit on $\mu_{H \rightarrow c\bar{c}}$, assuming SM production rates for $t\bar{t}H$ and VH, is 9.3 (5.6). For κ_c , the combination improves the expected 95% CL interval to $|\kappa_c| < 2.7$, while the observed is $|\kappa_c| < 3.5$. This represents the most stringent constraint on κ_c to date.

References

1. ATLAS Collaboration. *JINST*, 3:S08003, 2008.
2. CMS Collaboration. *JINST*, 3:S08004, 2008.
3. ATLAS Collaboration. *Phys. Lett. B*, 716:1, 2012.
4. CMS Collaboration. *Phys. Lett. B*, 716:30, 2012.
5. CMS Collaboration. *Phys. Lett. B*, 805:135425, 2020.
6. CMS Collaboration. *Nature*, 607:60, 2022.
7. ATLAS Collaboration. *Nature*, 607(7917):52–59, 2022. [Erratum: *Nature* 612, E24

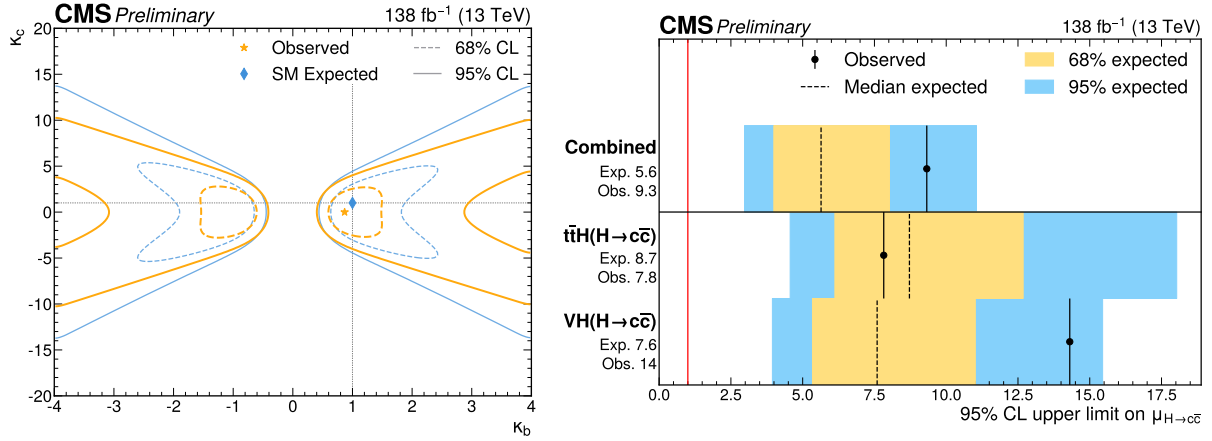


Figure 3 – Constraints on the Higgs boson coupling modifiers κ_c and κ_b (left) and the 95% CL upper limits on $\mu_{H \rightarrow c\bar{c}}$ (right)¹³.

(2022)].

8. CMS Collaboration. *Phys. Rev. Lett.*, 122:021801, 2019.
9. ATLAS Collaboration. Measurements of WH and ZH production with Higgs boson decays into bottom quarks and direct constraints on the charm Yukawa coupling in 13 TeV pp collisions with the ATLAS detector. Submitted to *JHEP*, 2024.
10. CMS Collaboration. *Phys. Rev. Lett.*, 131:061801, 2023.
11. Huilin Qu and Loukas Gouskos. *Phys. Rev. D*, 101:056019, 2020.
12. Emil Bols, Jan Kieseler, Mauro Verzetti, Markus Stoye, and Anna Stakia. *JINST*, 15:P12012, 2020.
13. CMS Collaboration. Search for Higgs boson decay to a charm quark-antiquark pair via $t\bar{t}H$ production, 2023. CMS-PAS-HIG-24-018 <https://cds.cern.ch/record/2929444>.
14. Huilin Qu, Congqiao Li, and Sitian Qian. Particle Transformer for jet tagging. In *Proceedings of the 39th International Conference on Machine Learning (ICML)*, Baltimore, USA, 2022. [PMLR 162:18281-18292].
15. CMS Collaboration. Inclusive and differential measurement of top quark cross sections in association with a z boson, 2024. CMS-PAS-TOP-23-004 <https://cds.cern.ch/record/2893862>.
16. ATLAS Collaboration. *JHEP*, 07:163, 2024.
17. LHC Higgs Cross Section Working Group. Handbook of LHC Higgs cross sections: 4. deciphering the nature of the Higgs sector. CERN Yellow Report, CERN, 2016. CERN-2017-002.